Ultrafast Photoinduced Charge Separation in Metal–Semiconductor Nanohybrids

Denis Mongin,[†] Ehud Shaviv,[‡] Paolo Maioli,[†] Aurélien Crut,[†] Uri Banin,[‡] Natalia Del Fatti,[†,*] and Fabrice Vallée[†]

[†]FemtoNanoOptics group, Université Lyon 1, CNRS, LASIM, 43 Bd du 11 Novembre, 69622 Villeurbanne, France, and [‡]Institute of Chemistry and the Center for Nanoscience and Nanotechnology, The Hebrew University of Jerusalem, Jerusalem 91904, Israel

ABSTRACT

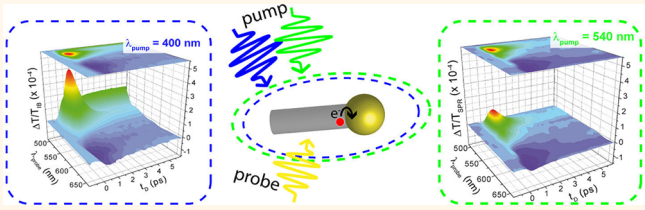

Hybrid nano-objects formed by two or more disparate materials are among the most promising and versatile nanosystems. A key parameter in their properties is interaction between their components. In this context we have investigated ultrafast charge separation in semiconductor–metal nanohybrids using a model system of gold-tipped CdS nanorods in a matchstick architecture. Experiments are performed using an optical time-resolved pump–probe technique, exciting either the semiconductor or the metal component of the particles, and probing the light-induced change of their optical response. Electron–hole pairs photoexcited in the semiconductor part of the nanohybrids are shown to undergo rapid charge separation with the electron transferred to the metal part on a sub-20 fs time scale. This ultrafast gold charging leads to a transient red-shift and broadening of the metal surface plasmon resonance, in agreement with results for free clusters but in contrast to observation for static charging of gold nanoparticles in liquid environments. Quantitative comparison with a theoretical model is in excellent agreement with the experimental results, confirming photoexcitation of one electron–hole pair per nanohybrid followed by ultrafast charge separation. The results also point to the utilization of such metal–semiconductor nanohybrids in light-harvesting applications and in photocatalysis.

KEYWORDS: hybrid nanoparticles · metal–semiconductor · CdS–Au nanocrystals · time-resolved spectroscopy · ultrafast processes · charge transfer · energy transfer

Fabrication and investigation of the novel properties of hybrid nano-objects formed by different inorganic materials are very active and quickly growing fields in nanoscience.[1−4] This interest is motivated by the wide range of possibilities offered by combination of two or more materials in a nano-object for designing multifunctional nanomaterials, combining the component material properties, or for creating new properties. In addition to the shape and size parameters, this can be done by controlling new parameters, e.g., adjusting the composition of the nanohybrids, their structure, or the interaction between the constituting materials. In this context investigating and understanding the interaction between the material components of hybrid nanoparticles are key issues for modeling their properties and for designing new ones.[5]

In the optical domain, metal-based hybrid nano-objects are particularly interesting as plasmonic effects can be combined with the optical response of the other component materials. In particular, metal–semiconductor nanohybrids offer the possibilities of combining plasmonics and quantum confinement effects and thus to lead to enhanced or quenched optical responses depending on the material interactions.[6−9] Recent advances in wet chemistry have permitted their controlled synthesis, opening many perspectives for their development.[1,2,4] Different fabrication approaches have been developed on the basis of either functionalization of one of the components to permit growth of the other one, or on direct growth of metal on a semiconductor nanoparticle (as for this work), creating a nanoscale junction.[6,10−12] This interfacing has been shown to modify the absorption spectra due to plasmon–exciton interaction and to either enhance or quench the semiconductor luminescence depending on the component spacing.[5,7,11−15] These effects reflect the underlying energy and charge transfer between the two material components. A key parameter is thus the metal–semiconductor interface, the presence of an intermediate layer deeply modifying the involved mechanisms.[1,16−19] While results on charge

* Address correspondence to natalia.del-fatti@univ-lyon1.fr.

Received for review May 11, 2012 and accepted July 15, 2012.

Published online July 16, 2012
10.1021/nn302089h

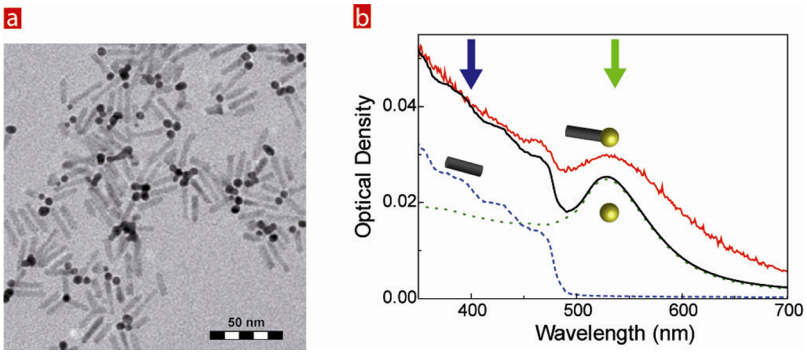

Figure 1. Linear optical properties of hybrid nanomatchsticks. (a) Transmission electron microscopy (TEM) micrograph of CdS−Au nanohybrids soluble in aqueous solution. The colloidal solution contains about 70% of nanomatchsticks (CdS nanorods terminated with a Au nanoparticle) and 30% of bare CdS nanorods. Mean sizes are: CdS length L = 23 nm, width W = 5 nm, Au diameter D = 6 nm. (b) Experimental absorption spectrum of the nanohybrid colloidal solution (red solid line, measured in 1 mm cuvette). Also shown are the measured absorption of an aqueous solution of bare CdS nanorods with same sizes and density (blue dashed line), and the computed absorption spectrum (green dotted line) of bare Au nanoparticles with concentration and shape dispersion similar to that in the nanohybrid solution (multipolar Mie theory has been used with a mean environment refractive index n_m = 1.43, and the dielectric function of gold[58] corrected for surface scattering effect). The black solid line is the sum of these two single-material spectra. The arrows indicate the different excitation wavelengths for time-resolved experiments.

transfer kinetics have been reported,[20,21] still little information has been obtained when the two materials are directly contacted, except in the presence of a large density of defects.[22]

Using time-resolved spectroscopy, we have investigated ultrafast charge and energy transfer kinetics in high quality CdS−Au matchstick nanohybrids formed by direct growth of a metal tip on a semiconductor nanorod.[23] Comparison of the results obtained in the nanohybrid colloidal solution to those in CdS nanorods or Au nanospheres solutions demonstrates ultrafast red-shift of the surface plasmon resonance of the gold part of the nanohybrid when photoexciting carriers in its semiconductor part. This is shown to be a signature of charging of the metal due to transfer of the electrons photoexcited in the semiconductor, in quantitative agreement with a theoretical model. In contrast to previous studies, where electron kinetics is probably dominated by the presence of defects,[22] ultrafast electron transfer is observed and is estimated to take place on a sub-20 fs time scale. This observation points to the utilization of hybrid semiconductor−metal nanoparticles in light-harvesting applications as they can provide, on the single-particle basis, both tunable absorption of the solar light and a rapid charge separation process. This provides important input for the further development of such systems as photocatalysts, as already demonstrated in the utilization of metal−semiconductor hybrids in photocatalytic water-splitting processes.[24−26]

RESULTS AND DISCUSSION

Linear Optical Properties. The investigated samples were synthesized by direct growth of Au nanoparticles on CdS nanorods. The synthesis procedure was described previously,[23] and more details are given in the Methods section. Briefly, CdS nanorods were first prepared using a "seeded growth" approach.[27,28] Part of the bare CdS nanorod solution was taken to provide a test solution for the time-resolved studies. Gold nanospheres were grown on the CdS rod tips using a photoinduced procedure.[23] The matchstick-shaped CdS−Au nanoparticles were transferred to the aqueous phase, providing the samples used in the time-resolved studies. Using this procedure most of the nanorods (about 70%) are decorated by a gold nanoparticle at one of their apexes, forming CdS−Au nanomatchsticks. Residual bare CdS nanorods are also present in the aqueous solution (about 30%) (Figure 1a). The mean length and width of the semiconductor nanorods are L = 23 nm and W = 5 nm respectively, and the mean gold tip diameter D = 6 nm.

The absorption spectrum of the nanohybrid colloidal solution (Figure 1b, red line) exhibits both the characteristic excitonic and continuous absorption of the CdS nanorods (for wavelengths around and below its band edge at about 480 nm), together with an additional broad resonance around 530 nm due to the gold nanospheres. The former is consistent with the absorption features of a solution of bare CdS nanorods (blue dashed line in Figure 1b). The latter corresponds to the characteristic localized surface plasmon resonance (SPR) of small metal nanospheres.[29] For comparison, the absorption spectrum of a colloidal solution of pure Au nanoparticles with mean diameter D = 6 nm, computed taking into account their concentration with shape, size, and environment dispersion as estimated in the nanohybrid solution, is plotted in Figure 1b (green dotted line). It exhibits the same features, with a SPR around 530 nm partly overlapping the gold interband transitions which dominate gold absorption at shorter wavelengths.[29−31]

As reported in a recent study[5] the sum of the extinction spectra of bare CdS and bare Au nanoparticles (Figure 1b, black line) is close to the one of the hybrid

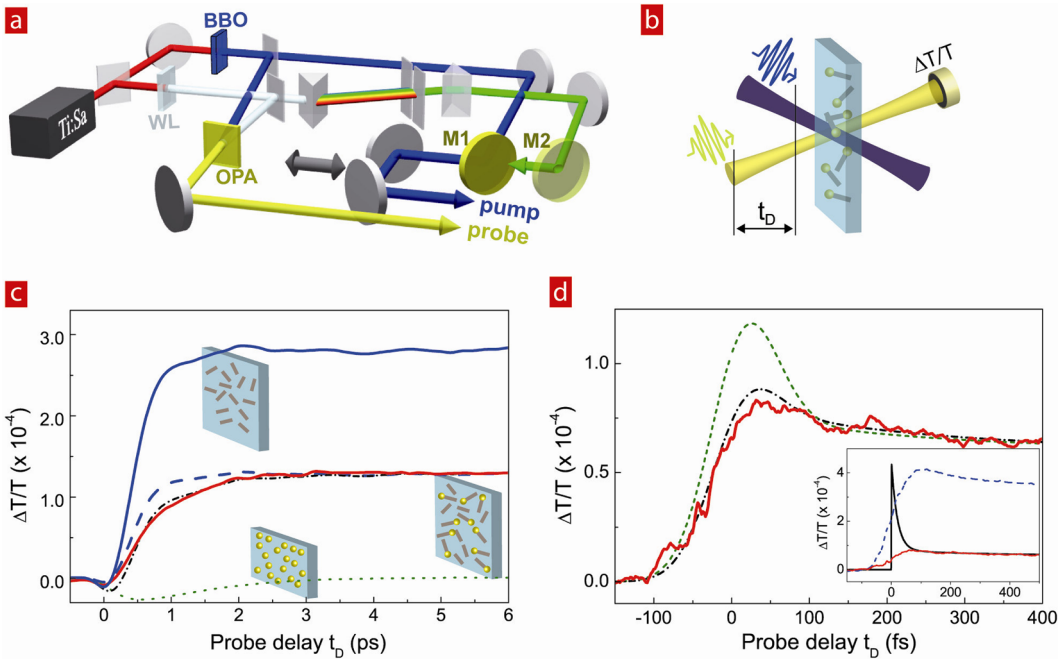

Figure 2. Charge transfer in semiconductor−metal nanohybrids: probing the CdS nanorods. (a) Schematic setup for ultrafast nonlinear investigations, showing the amplified femtosecond laser with nonlinear frequency conversions: second harmonic generation in a BBO crystal, supercontinuum white light (WL) generation and optical parametric amplification (OPA). (b) Principle of a time-resolved pump−probe optical experiment. (c) Time-dependent transmission change $\Delta T/T$ measured in bare CdS nanorods (blue solid line) and CdS−Au nanomatchstick solution (red solid line) for pump and probe wavelengths λ_{pump} = 400 nm and λ_{probe} = 480 nm, respectively. The pump energy is about 200 pJ per pulse. The CdS−Au nanohybrid response is well reproduced by the sum (black dash−dotted line) of the contributions of gold (green dotted line) and CdS (blue dashed line, obtained by multiplying the bare CdS nanorods signal by a reduction factor, which permits estimation that 75% of the nanohybrids exhibit photoexcited charge separation). (d) Short time delay transmission change $\Delta T/T$ measured in CdS−Au nanomatchstick solution (red solid line) for a degenerate pump−probe experiment with pulse durations of 38 fs and $\lambda_{pump} = \lambda_{probe}$ = 450 nm. The lines are computed by convoluting the pump−probe optical cross-correlation (see Supporting Information) with a hybrid response corresponding to an electron transfer time of 20 fs (green dashed line) and 10 fs (black dash-dotted line). This impulsive response is shown in the inset (black solid line). Its maximum and minimum amplitudes are set by the signals in bare CdS (blue dotted line) and CdS−Au nanohybrid (red solid line) solutions, respectively, and the decay time constant is the electron transfer time.

solution. The difference between the two spectra is ascribed to the interaction within the two nanohybrid components. Hence, in the case of CdS−Au metal−semiconductor nanohybrids the optical properties of the original components are essentially retained. This is attributed to the spectral separation of the optical excitations of the metal and the semiconductor parts in this hybrid system, making them weakly interacting.[5] The separation of the excitonic and plasmonic features in CdS−Au nanohybrids has the advantage of enabling selective time-domain excitation and probing of their material components using two-color femtosecond pump−probe spectroscopy (Figure 2).

Ultrafast Time-Resolved Pump−Probe Experiments. In these experiments, a femtosecond pump pulse, with wavelength λ_{pump}, is first used to excite the hybrid nanoparticles. Tuning λ_{pump} around the gold SPR (*i.e.*, $\approx$ 540 nm) only the gold part is excited, while both components are photoexcited for λ_{pump} below the CdS band gap (see Figure 1b). Probing the relative optical transmission change, $\Delta T/T$, of the sample with a time-delayed probe pulse, with wavelength λ_{probe}, permits to monitor energy and charge redistribution in the nanohybrid (Figure 2b). More precisely the time-dependent density of photoexcited carriers in the semiconductor part can be monitored for λ_{probe} below the CdS band gap (with a smaller contribution due to the transient change of the gold part), while both gold heating and charging are monitored when probing with wavelengths around the SPR.

The two-color pump and probe femtosecond pulses are provided by a Ti:sapphire regenerative amplifier delivering 100 fs pulses at 800 nm with a repetition rate of 250 kHz associated to an optical parametric amplifier (OPA) system (Figure 2a). The output pulse train is split into two parts, one being frequency-doubled to 400 nm in a 200 μm thick BBO crystal. The second one is focused in a sapphire plate to generate a white-light supercontinuum. The pump pulses are either at 400 nm (using part of the frequency-doubled beam) or 540 nm (frequency selecting part of the supercontinuum), corresponding to positions M1 or M2 of the optical mirror in Figure 2a, respectively. The wavelength tunable probe pulses are created by optical parametric amplification of part of the supercontinuum (with a full-width at half-maximum

of about 5 nm) in a second nonlinear BBO crystal pumped by the frequency doubled pulses. The temporal resolution of the system is given by the pump−probe cross-correlation and is about 150 fs (for further details on the experimental setup and pulse durations see Supporting Information). The time delay t_D between the pump and probe pulses is adjusted using a mechanical delay stage on the pump beam path. High sensitivity detection of the pump-induced changes is achieved by mechanical chopping of the pump beam at 40 kHz and lock-in detection of the probe transmission change.

The Semiconductor Nonlinear Response. To investigate the dynamics of the photoexcited carriers in the semiconductor part, experiments were first performed using a pump photon energy above the CdS band gap, λ_{pump} = 400 nm, and probing close to the band gap, λ_{probe} = 480 nm, either in the bare CdS nanorod solution or in the matchstick one. A low incident pump power (about 50 μW, i.e. 200 pJ per pulse) was used to excite on the average less than one electron−hole pair per CdS nanorod (the mean value is about 0.8 e-h pair per rod). Experiments performed in the test sample formed by bare CdS nanorods in solution show absorption bleaching assigned to carrier state filling (Figure 2c, blue solid line).[32,33] As expected, after a rise reflecting electron photoexcitation and intraband relaxation, the $\Delta T/T$ signal reaches a plateau (Figure 2c, blue solid line) that decays on a few hundred picosecond time scale reflecting electron density decay due to carrier recombination and electron trapping (a signal measured on a longer time scale is reported in Figure S2 of Supporting Information). Similar results are obtained for different probe wavelengths close to the CdS band-edge, in agreement with previous experiments in confined semiconductors.[32,33] To characterize the effect of coupling with metal on the semiconductor dynamics, the same experiment was repeated on the nanohybrid sample, the amplitude of the signal being subsequently normalized to the same pump energy absorbed by each CdS nanorod (Figure 2c, red solid line). Comparison of the two curves after normalization proves a weaker $\Delta T/T$ signal bleach amplitude in the nanohybrid sample. This reduced bleaching demonstrates that, on the investigated time scale, the density of photoexcited carriers in the semiconductor nanorods is reduced when they are contacted with metal nanoparticles. This indicates ultrafast semiconductor to metal photoexcited electrons transfer, on a time-scale much smaller than the time-resolution of our experimental setup. More quantitatively, for the used probe wavelength (λ_{probe} = 480 nm) the measured $\Delta T/T$ signal is the sum of the optical response of the gold part of the nanohybrids, and of the CdS nanorods which have not transferred their charge. Actually, as less than one electron is photoexcited per CdS nanorod, the gold-decorated ones are not showing absorption bleaching after transferring their photoexcited electron to the gold part. This is based on the understanding that the main source of bleach for the CdS rods arises from state filling of the conduction band electron states. In bulk semiconductors, because of the difference between the electron and hole effective masses, the valence band distribution is much broader in momentum space than that of the corresponding conduction band and therefore, for small wave vectors, the electron occupation number is much larger than the hole one.[34−36] When probing close to the band edge, state filling is therefore essentially dominated by the occupation of the conduction band states.[34,37] Similar results are expected in the case of confined systems,[32,33]the level structure at the valence band for the holes being much more dense on account of the heavier effective mass and band-mixing effects. This was also nicely demonstrated for CdS and CdSe/CdS quantum dots in the presence of an electron acceptor, which led to significant decrease in the measured bleach.[38] The main residual bleaching is thus due to the bare CdS nanorods left in the solution (see Figure 1a) or to nanohybrids not exhibiting charge transfer. In the probed spectral region ($\lambda_{probe} \leq$ 480 nm), the signal from Au nanoparticles only leads to a weak induced absorption, as expected from previous experiments[39] and confirmed by repeating the pump−probe measurement on a bare gold nanosphere solution (Figure 2c, green dotted line), after normalization of the signal to the same pump energy absorbed by gold. The experimental $\Delta T/T$ amplitude and time evolution of the nanohybrid solution (red solid line) is thus very well reproduced as the sum (black dash-dotted line) of the weak gold response (green dotted line) and of the absorption bleaching of all the residual bare CdS semiconductors and of about 25% of the CdS−Au matchsticks (blue dashed line, obtained by multiplying the blue solid line by a reduction factor). This suggests that charge transfer occurs in about 75% of the nanomatchsticks but not in the remaining ones, possibly because of poor CdS−Au interfacial contact or to electron localization in the semiconductor due to surface traps.

To estimate the CdS−Au electron transfer time, similar experiments were performed in a degenerated pump−probe configuration ($\lambda_{pump} = \lambda_{probe}$ = 450 nm) using shorter pulses ($\approx$ 38 fs) delivered by a home-made frequency doubled Ti:Sapphire oscillator (for further details on the setup see Figure S1 in Supporting Information). As before, in this configuration the $\Delta T/T$ signal directly probes the semiconductor electron density, but as the same pump and prove wavelengths are used, the excited and probed semiconductor states are identical. Observation of a transient $\Delta T/T$ peak due to transient population of the electronic states is thus expected if charge transfer is slower or of the order of the pulse duration. No marked peak is observed experimentally suggesting fast charge transfer time.

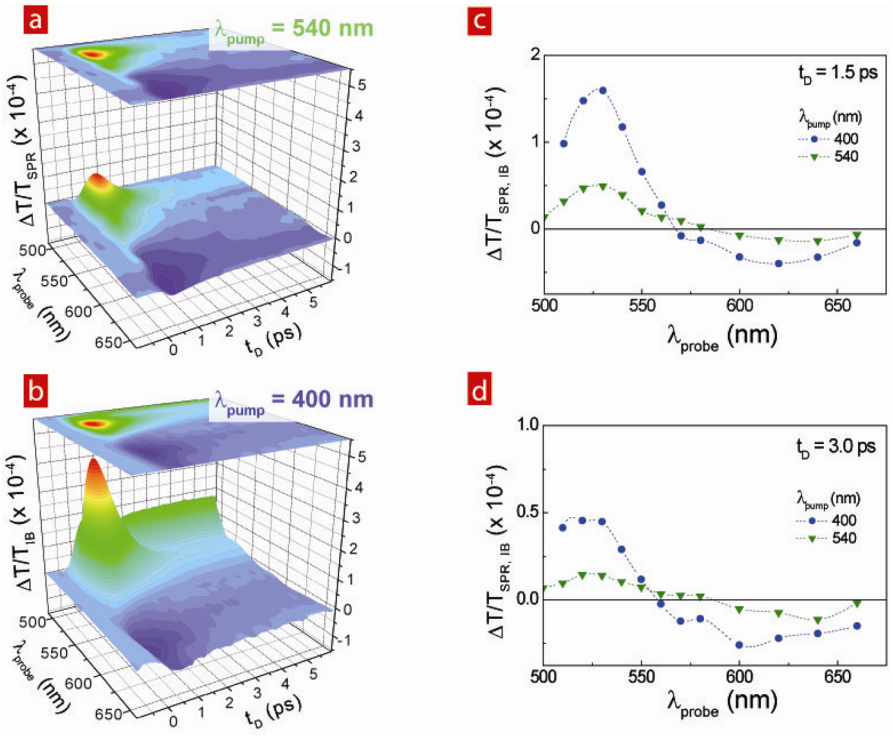

Figure 3. Ultrafast response of semiconductor−metal nanohybrids: probing the Au nanoparticles. Time and spectrally resolved transmission change $\Delta T/T(t_{Dprobe}\lambda_{probe})$ measured in CdS−Au nanomatchsticks solution for a pump wavelength (a) λ_{pump} = 540 nm (close to the surface plasmon resonance of gold nanoparticles: $\Delta T/T_{SPR}$) and (b) λ_{pump} = 400 nm (below the CdS band gap and gold interband transition threshold: $\Delta T/T_{IB}$). The data are normalized to the same amount of absorbed energy in the gold nanoparticles. The $\Delta T/T_{IB}$ signal for λ_{probe} < 500 nm is dominated by the CdS response (Figure 2c) and is not shown here. (c) Experimental spectral transmission changes $(\Delta T/T)_{IB,\ SPR}$ (λ_{probe}) for λ_{pump} = 400 nm (blue dots, from b) and λ_{pump} = 540 nm (green triangles, from a) at a fixed pump−probe delay t_D = 1.5 ps. (d) Same as (c) at a fixed pump−probe delay t_D = 3 ps.

To estimate its upper limit, the photoexcited electron density in the CdS rods has been assumed to decay monoexponentially. Convoluting this response with the experimental pump−probe cross-correlation, the short time-behavior of $\Delta T/T$ can only be reproduced assuming an electron density decay time, i.e., charge transfer time, shorter than about 20 fs (Figure 2d). This transfer time is much faster than that reported in the presence of an interfacial layer between the semiconductor and metal component or in the presence of interfacial defects.[22] However, it is consistent with the fastest times measured in other hybrid systems such as dye molecules contacted with a semiconductor dot in hybrid solar cells, when the molecules are directly interacting with the dots.[40−43]

The Metal Nonlinear Response. To further confirm ultrafast CdS−Au electronic transfer, we have monitored the transient change of the optical response of the hybrid nanomatchsticks in a spectral region dominated by their gold part, i.e., close to the gold SPR (wavelengths longer than the CdS band-edge, Figure 1). For probe wavelengths in this spectral region, the transient transmission change $\Delta T/T$ contains contributions both from direct heating of the electrons of the gold part by the pump beam and from indirect excitation *via* photoexcitation of the semiconductor part. The latter mechanism can be singled out by comparing the results of two series of pump−probe experiments performed with or without exciting the CdS part of the nanohybrids. This can be done using a pump photon energy above the CdS band gap λ_{pump} = 400 nm, or below it, close to the gold SPR, λ_{pump} = 540 nm (Figure 1b). The time and spectral dependence of the nanohybrid transmission changes close and above the gold SPR wavelength (λ_{probe} > 500 nm) are shown in Figure 3 for the two excitation conditions ($(\Delta T/T)_{IB}$ and $(\Delta T/T)_{SPR}$ are measured with λ_{pump} = 400 nm and with λ_{pump} = 540 nm, respectively, and normalized to the same absorbed energy in the gold part of the nanomatchsticks). When exciting only the metal part of the nanohybrid (λ_{pump} = 540 nm), transmission is found to increase ($\Delta T/T > 0$) when probing close to the SPR wavelength and to decrease ($\Delta T/T < 0$) away from it (Figure 3a). This behavior is in very good agreement with previous studies in gold nanoparticles and reflects heating of the gold electrons by the pump pulse.[39] The $\Delta T/T$ signal-decays reflect cooling of the hot electrons to the lattice with a time constant τ_{e-L} of about 1 ps, as previously reported in gold nanoparticles of similar size in the weak excitation regime.[44] For excitation energy above the excitonic band-edge (λ_{pump} = 400 nm), a larger transient transmission change amplitude is

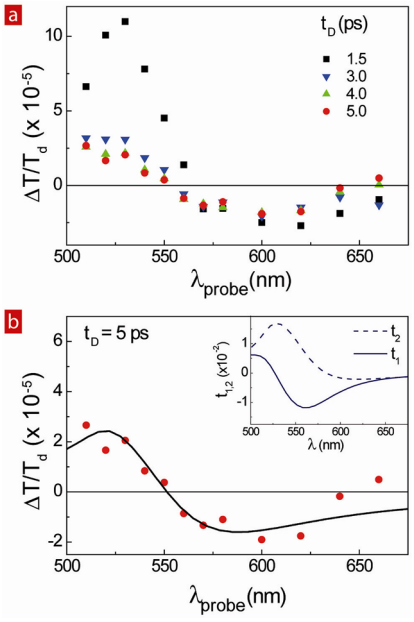

Figure 4. Ultrafast spectral response of the charged Au nanoparticles. (a) Spectral dependence of the difference of the transmission changes $(\Delta T/T)_d = (\Delta T/T)_{IB} - (\Delta T/T)_{SPR}$ measured for pump wavelength λ_{pump} = 400 and 540 nm (from Figure 3) in CdS−Au nanomatchsticks for different time delays t_D. (b) Experimental $(\Delta T/T)_d$ signal for t_D = 5 ps together with a fit (solid line) taking into account semiconductor−metal electron and energy transfer within the CdS−Au nanohybrids. The inset shows the coefficients t_1 (solid line) and t_2 (dashed line) used in the model (see text).

observed together with modification of its shape around the SPR (Figure 3b) (a positive contribution also shows-up for the shortest probe wavelengths, $\lambda_{probe} \leq 500$ nm, due to the onset of the semiconductor band filling response as shown in Figure 2). The two different responses are better compared by plotting the $\Delta T/T$ spectra at fixed pump−probe delays (t_D = 1.5 ps in Figure 3c and t_D = 3 ps in Figure 3d), clearly showing a shift of the wavelength at which $\Delta T/T$ exhibits a sign-change. These spectral and amplitude changes are consequences of photoexcitation of the semiconductor part of the nanohybrids on the transient response of their gold part.

In order to single out these consequences, the contribution of direct heating of the gold electrons by the pump pulse has been removed by subtracting the signal measured for gold excitation only (λ_{pump} = 540 nm) from that for both gold and CdS excitation (λ_{pump} = 400 nm): $(\Delta T/T)_d = (\Delta T/T)_{IB} - (\Delta T/T)_{SPR}$ (for a fixed pump−probe delays and after signal normalization to the same absorbed energy in the gold part, Figure 4a). This approach is justified in the weak excitation regime used here, as $\Delta T/T$ scales linearly with the excitation amplitude, and after about 100 fs, the spectral and temporal shapes of the transient response of a metallic nanoparticle due to direct electron heating is independent of the pump wavelength (it only depends on the deposited energy in the conduction electrons).[45] The differential transmission, $(\Delta T/T)_d$, exhibits a transient large amplitude for short time delays ($t_D \leq 2-3$ ps), characteristic of additional ultrafast gold electron heating. As expected this feature decays with the electron−lattice energy exchange time of gold τ_{e-L}, leading to an electron−lattice thermalized gold particle (after 2−3 ps) at a temperature larger than for the no-CdS excitation case. In this quasi-equilibrium regime, reduced differential transmission, $(\Delta T/T)_d$, is observed on the red side of the gold SPR, indicating a red-shift of the SPR, signature of charging of the gold particle (see below). We will focus on this quasi-equilibrium regime, as the impact of both gold heating and charging can be quantitatively modeled. Connecting the measured $(\Delta T/T)_d$ to the change of the metal dielectric function $\Delta\varepsilon$, changes of the gold temperature and electron density due to photoexcitation of the semiconductor part can thus be estimated.

In the small perturbation regime used here, the transmission changes of a gold nanoparticle is a linear combination of the changes of the real, $\Delta\varepsilon_1$, and imaginary, $\Delta\varepsilon_2$, part of ε:

$$\Delta T/T = t_1\Delta\varepsilon_1 + t_2\Delta\varepsilon_2 \quad (1)$$

As done before,[46,47] the coefficients $t_{1,2} = \partial \ln T/\partial\varepsilon_{1,2}$ can be numerically computed from the gold contribution to the linear optical response, taking into account only the fraction of nanohybrids which shows charge transfer (Figure 4b, inset). After electron−lattice relaxation (i.e., $t_D \geq 3$ ps), modification of the metal dielectric function is mainly due to changes of its Drude part: $\varepsilon_{Drude} = 1 - \omega_p^2/\omega(\omega + i\gamma)$, where $\omega_p^2 = ne^2/\varepsilon_0 m_e$ is the plasma frequency.[47] Nanoparticle heating and change of its electron density n translate in modifications of the optical electron scattering rate, γ, and of ω_p. The former mostly leads to a ε_2 change and the latter to a ε_1 change, i.e., to $(\Delta T/T)_d$ signals proportional to t_2 and t_1, respectively (approximately corresponding to a SPR broadening and spectral shift):

$$\Delta\varepsilon_2 = \frac{\omega_p^2}{\omega^3}\Delta\gamma;\ \Delta\varepsilon_1 = -\frac{\omega_p^2}{n\omega^2}\Delta n \quad (2)$$

Using this approach and $\Delta\gamma$ and Δn as parameters, a good reproduction of the long delay differential transmission $(\Delta T/T)_d$ is obtained with $\Delta\gamma/\gamma \approx 1.1 \times 10^{-3}$ and $\Delta n/n \approx -5 \times 10^{-5}$ (Figure 4b). As for the $(\Delta T/T)_d$ amplitude and shape (Figure 4a), these values are constant over the investigated time scale (about 6 ps), indicating gold particle neutralization and cooling on a much longer time-scale.[48]

The estimated reduction of the electron density in the gold particle (negative value of Δn) is correlated to the observed red-shift of the SPR. This reduction might seem surprising, as the presence of an additional electron in the gold part of the nanohybrid is expected. However, it is consistent with the experimental and theoretical studies performed in noble-metal clusters

in vacuum.[49,50] In these conditions, it has been demonstrated that negatively charging a free cluster leads to a net decrease of its electronic density, due to the concomitant increase of its electronic radius, r_e. The latter effect reflects increase of the Coulombic repulsion and thus of the spill-out effect (as a result of the finite electron confinement potential in a nanoparticle, the electronic wave functions extend beyond the ionic core, *i.e.* $r_e > R$, this spill-out effect increasing with additional Coulombic repulsion). The net change of the electronic density $n = N/(4/3\pi r_e^3)$ is thus a balance between increase of the number of electrons and of the volume they occupy. Following the results obtained in free clusters, the change of the spill-out effect for singly charged noble metal nanoparticles is of the order of $\Delta r_e/r_e \approx 1.8 \times 10^{-3}$ nm^3/R^3.[51] For a $R = 3$ nm radius gold nanoparticle (with $N \approx 6700$ electrons) adding one electron thus leads to small reduction of the electron density $\Delta n/n = 1/N - 3\Delta r_e/r_e \approx -5.10^{-5}$, in excellent agreement with our results.

This electron density reduction observed on a few picoseconds time scale for a negatively charged gold particle is in contrast to the results obtained for static charging of gold particles in solution showing a blue-shift of the gold SPR.[52−54] In these experiments, charge transfer is either photoinduced from semiconductor nanostructures or induced by chemisorption at the nanoparticle surfaces or by static electrochemical charging of the metal particles (see for instance Kamat *et al.*[54] and Warren *et al.*[55]). As long time scales are involved, the nanoparticles are in equilibrium with their close environment, strongly influencing the observed change of the SPR position. The role of the environment has been recently demonstrated by performing static charging experiments on a single gold nanorod, a blue-shift being observed for negative potentials in the presence of aqueous and different salt solutions, while no shift is observed in air (probably because of the smallness of the intrinsic effect due only to the particle electron density change[56]). These different behaviors have to be ascribed to rearrangement of the solvent and surfactant molecules upon particle charging. Such an effect is absent in our short time scale measurements, the environment being unchanged on a few picoseconds. Environmental effect can thus be neglected, and as for free clusters, only the fast electronic processes in the nanoparticles are observed, leading to the detected small red-shift of the gold SPR. Furthermore, we also emphasized that in static charging experiments in solution a few thousands of electrons are expected to be exchanged,[53,55] while only one electron is added per gold particle in our present study. This very different regime also translates into a measurement of much smaller SPR spectral shifts (a few tens of μeV), as compared to the large ones usually observed in static experiments (a few tens of meV).

The observed increase of the electron damping rate, γ, reflects additional heating of the gold particles. This is ascribed to energy transfer concomitant with arrival of a photoexcited electron. Taking into account the pump photon energy and band structures of CdS nanorod and Au, the electron is estimated to be transferred in the metal conduction band with an excess energy of about 1.8 eV. After electron−lattice thermalization, this leads to an additional increase of the gold nanoparticle temperature of about 0.6 K.[47] Using the static temperature dependence of γ in bulk gold, $d\gamma/dT \approx 0.11$ meV/K[57] and its room temperature value $\hbar\gamma \approx 70$ meV,[58] this temperature rise translates into a relative change of the electron scattering rate $\Delta\gamma/\gamma \approx 1 \times 10^{-3}$. This is again in excellent agreement with the value deduced from fitting $(\Delta T/T)_d$, indicating ultrafast transfer of the nonequilibrium electron photoexcited in the semiconductor part of the nanohybrid particles to their metal part, together with their excess energy. Note that, due to the energy difference between the Fermi level of metal and the semiconductor conduction band,[8] the transfer of a photoexcited electron is always accompanied by an extra amount of energy transferred to the gold component, even for an excitation resonant with the semiconductor gap.

Our results are in contrast with those previously reported in other CdS−Au nanohybrids.[22] In these previous studies, the gold SPR features in the absorption spectra of nanohybrids were absent, conversely to theoretical expectation and experimental results reported elsewhere.[11,23,59] This absence of gold SPR-related absorption suggests that trap state effects dominate the measured optical responses. These traps also probably inhibit the fast charge and energy transfer that we have conversely measured in our samples, where both SPR and excitonic features are clearly observed. This suppression is also consistent with the absence of charge transfer for part of our CdS−Au nanomatchsticks (only about 75% of them being estimated to lead to charge transfer, Figure 2c).

CONCLUSION

In summary, using two-color pump−probe spectroscopy we have investigated energy and charge transfer in semiconductor−metal hybrid nanoparticles: CdS−Au nanomatchsticks. Their exciton and surface plasmon resonance being energetically separated, measurements were performed probing either the semiconductor or gold part for different excitation conditions. The results show ultrafast transfer of one photoexcited electron from the CdS to the Au component of the nanohybrid on a sub-20 fs time scale. This fast transfer is probably at the origin of the strong semiconductor luminescence quenching observed in this type of metal−semiconductor nanohybrid. Charging of the gold part of the nanomatchstick is shown to induce an ultrafast red-shift of the gold surface

plasmon resonance. This is in excellent agreement with free cluster experimental and theoretical studies, but in contrast with the results of static charging experiments, probably due to the absence of environmental effects, such as molecular absorption or desorption at the surface of the particles, on a few picoseconds time scale.

Extension of these measurements to the resonant exciton–surface plasmon situation, as in CdSe–Au, would bring new insights on the impact of material excitation coupling on nanohybrid properties. More generally, these studies open up many possibilities for the investigation of the impact of different material coupling on the linear and nonlinear optical properties of hybrid nano-objects. The observation of ultrafast light-induced charge separation in such hybrids motivates further studies of their utilization in light-harvesting applications.

METHODS

Synthesis of the CdS nanorods. CdS nanorods were grown by utilizing a "seeded growth" approach.[27,28] Herein is a brief description of the typical procedure for making these nanorods.

A solution containing sulfur precursor and the seeds was prepared by dissolving 4×10^{-8} mole of 2.5 nm CdS quantum dots in 1.6 mL trioctylphosphine (TOP 97%) together with 120 mg sulfur powder. In a separate flask, 30 mg cadmium oxide (CdO 99.9%), 150 mg octadecylphosphonic acid (ODPA), 18 mg hexylphosphonic acid (HPA), and 3 g trioctylphosphine oxide (TOPO 99%) were dried under vacuum at 150 °C for an hour. Next, the temperature was raised to 360 °C under argon, and 0.5 mL TOP (97%) was added to the flask. The solution containing the seeds was rapidly injected to the flask under vigorous stirring. The reaction was left to take place at 360 °C for 5 min before removing the heating mantle.

Synthesis of the CdS–Au nanomatchsticks. The matchstick-shaped CdS–Au sample was prepared on the basis of the photoinduced procedure reported previously.[23] The CdS nanorods were cleaned from access ligands by methanol addition followed by centrifugation. The supernatant was discarded, and the precipitate was dissolved in 3 mL of toluene. The estimated concentration of nanorods was $\sim 1.2 \times 10^{-7}$ M (optical density OD $\approx$ 1.1 at 460 nm, the exciton band edge absorption peak). Next, a Au growth solution was prepared by dissolving 7.5 mg Au(III) chloride ($AuCl_3$ 99%, kept in dry conditions), 12 mg of didodecyldimethylammonium bromide (DDAB, 98%), and 35 mg of dodecylamine (DDA, 98%) in 6 mL toluene. Both the CdS and Au solutions were sonicated in sealed vials for 5 min and purged with argon for 5 min to remove oxygen from the reaction. Finally, the nanorods solution was placed in an ice bath ($T < 5$ °C) to suppress Au growth on defect sites, and 1 mL of Au growth solution was added into the vial under vigorous stirring. During the Au growth stage the vial was irradiated with a blue Neon lamp (20 W) in order to increase the growth rate. The reaction was stopped after 10 min of irradiation by precipitating the nanoparticles with acetone followed by centrifugation.

In order to prevent aggregation of the CdS–Au nanoparticles in the organic phase, after a few hours the sample was transferred to aqueous phase where it remained stable for days. This was performed by surface ligand exchange with mercaptoundecanoic acid (MUA 99%).

Conflict of Interest: The authors declare no competing financial interest.

Acknowledgment. We are grateful for funding from Nano-Sci ERA-Net under the program Single-NanoHybrid. N.D.F. acknowledges support by Institut Universitaire de France (IUF). U.B. thanks the Alfred & Erica Larisch Memorial Chair.

Supporting Information Available: Details of the pump–probe time-resolved transient absorption experiments and long-time dynamics measured in bare CdS nanorods. This material is available free of charge *via* the Internet at http://pubs.acs.org.

REFERENCES AND NOTES

1. Costi, R.; Saunders, A. E.; Banin, U. Colloidal Hybrid Nanostructures: A New Type of Functional Materials. *Angew. Chem., Int. Ed.* **2010**, *49*, 4878–4897.
2. Carbone, L.; Cozzoli, P. D. Colloidal Heterostructured Nanocrystals: Synthesis and Growth Mechanisms. *Nano Today* **2010**, *5*, 449–493.
3. Krahne, R.; Morello, G.; Figuerola, A.; George, C.; Deka, S.; Manna, L. Physical Properties of Elongated Inorganic Nanoparticles. *Phys. Rep.* **2011**, *501*, 75–221.
4. Vaneski, A.; Susha, A. S.; Rodríguez-Fernández, J.; Berr, M.; Jäckel, F.; Feldmann, J.; Rogach, A. L. Hybrid Colloidal Heterostructures of Anisotropic Semiconductor Nanocrystals Decorated with Noble Metals: Synthesis and Function. *Adv. Funct. Mater.* **2011**, *21*, 1547–1556.
5. Shaviv, E.; Schubert, O.; Alves-Santos, M.; Goldoni, G.; Di Felice, R.; Vallée, F.; Del Fatti, N.; Banin, U.; Sönnichsen, C. Absorption Properties of Metal-Semiconductor Hybrid Nanoparticles. *ACS Nano* **2011**, *5*, 4712–4719.
6. Mokari, T.; Rothenberg, E.; Popov, I.; Costi, R.; Banin, U. Selective Growth of Metal Tips onto Semiconductor Quantum Rods and Tetrapods. *Science* **2004**, *304*, 1787–1790.
7. Lee, J.; Govorov, A. O.; Dulka, J.; Kotov, N. A. Bioconjugates of CdTe Nanowires and Au Nanoparticles: Plasmon–Exciton Interactions, Luminescence Enhancement, and Collective Effects. *Nano Lett.* **2004**, *4*, 2323–2330.
8. Lin, H. Y.; Chen, Y. F.; Wu, J. G.; Wang, D. I.; Chen, C. C. Carrier Transfer Induced Photoluminescence Change in Metal-Semiconductor Core-Shell Nanostructures. *Appl. Phys. Lett.* **2006**, *88*, 161911.
9. Lee, J.; Javed, T.; Skeini, T.; Govorov, A. O.; Bryant, G. W.; Kotov, N. A. Bioconjugated Ag Nanoparticles and CdTe Nanowires: Metamaterials with Field-Enhanced Light Absorption. *Angew. Chem., Int. Ed.* **2006**, *45*, 4819–4823.
10. Mokari, T.; Sztrum, C. G.; Salant, A.; Rabani, E.; Banin, U. Formation of Asymmetric One-Sided Metal-Tipped Semiconductor Nanocrystal Dots and Rods. *Nat. Mater.* **2005**, *4*, 855–863.
11. Saunders, A. E.; Popov, I.; Banin, U. Synthesis of Hybrid CdS-Au Colloidal Nanostructures. *J. Phys. Chem. B* **2006**, *110*, 25421–25429.
12. Majimel, J.; Bacinello, D.; Durand, E.; Vallée, F.; Tréguer-Delapierre, M. Synthesis of Hybrid Gold-Gold Sulfide Colloidal Particles. *Langmuir* **2008**, *24*, 4289–4294.
13. Larkin, I.; Stockman, M.; Achermann, M.; Klimov, V. I. Dipolar Emitters at Nanoscale Proximity of Metal Surfaces: Giant Enhancement of Relaxation in Microscopic Theory. *Phys. Rev. B* **2004**, *69*, 121403(R).
14. Pustovit, V.; Shahbazyan, T. V. Resonance Energy Transfer Near Metal Nanostructures Mediated by Surface Plasmons. *Phys. Rev. B* **2011**, *83*, 085427.
15. Shi, W.; Zeng, H.; Sahoo, Y.; Ohulchanskyy, T. Y.; Ding, Y.; Wang, Z. L.; Swihart, M.; Prasad, P. N. A General Approach to Binary and Ternary Hybrid Nanocrystals. *Nano Lett.* **2006**, *6*, 875–881.
16. Liu, N.; Prall, B. S.; Klimov, V. I. Hybrid Gold/Silica/Nanocrystal-Quantum-Dot Superstructures: Synthesis and Analysis of

Semiconductor-Metal Interactions. *J. Am. Chem. Soc.* **2006**, *128*, 15362–15363.
17. Haldar, K. K.; Sen, T.; Patra, A. Metal Conjugated Semiconductor Hybrid Nanoparticle-Based Fluorescence Resonance Energy Transfer. *J. Phys. Chem. C* **2010**, *114*, 4869–4874.
18. Fedutik, Y.; Temnov, V.; Woggon, U.; Ustinovich, E.; Artemyev, M. Exciton-Plasmon Interaction in a Composite Metal-Insulator-Semiconductor Nanowire System. *J. Am. Chem. Soc.* **2007**, *129*, 14939–14945.
19. Wang, Q.; Wang, H.; Lin, C.; Sharma, J.; Zou, S.; Liu, Y. Photonic Interaction between Quantum Dots and Gold Nanoparticles in Discrete Nanostructures through DNA Directed Self-Assembly. *Chem. Commun.* **2010**, *46*, 240–242.
20. Achermann, M. Exciton−Plasmon Interactions in Metal−Semiconductor Nanostructures. *J. Phys. Chem. Lett.* **2010**, *1*, 2837–2843.
21. Berr, M. J.; Vaneski, A.; Mauser, C.; Fischbach, S.; Susha, A. S.; Rogach, A. L.; Jäckel, F.; Feldmann, J. Delayed Photoelectron Transfer in Pt-Decorated CdS Nanorods under Hydrogen Generation Conditions. *Small* **2011**, *8*, 291–297.
22. Khon, E.; Mereshchenko, A.; Tarnovsky, A. N.; Acharya, K.; Klinkova, A.; Hewa-Kasakarage, N. N.; Nemitz, I.; Zamkov, M. Suppression of the Plasmon Resonance in Au/CdS Colloidal Nanocomposites. *Nano Lett.* **2011**, *11*, 1792–1799.
23. Menagen, G.; Macdonald, J. E.; Shemesh, Y.; Popov, I.; Banin, U. Au Growth on Semiconductor Nanorods: Photoinduced *Versus* Thermal Growth Mechanisms. *J. Am. Chem. Soc.* **2009**, *131*, 17406–17411.
24. Berr, M.; Vaneski, A.; Susha, A. S.; Rodríguez-Fernández, J.; Doblinger, M.; Jäckel, F.; Rogach, A. L.; Feldmann, J. Colloidal CdS Nanorods Decorated with Subnanometer Sized Pt Clusters for Photocatalytic Hydrogen Generation. *Appl. Phys. Lett.* **2010**, *97*, 093108.
25. Shemesh, Y.; Macdonald, J. E.; Menagen, G.; Banin, U. Synthesis and Photocatalytic Properties of a Family of CdS-PdX Hybrid Nanoparticles. *Angew. Chem.* **2011**, *123*, 1217–1221.
26. Amirav, L.; Alivisatos, A. P. Photocatalytic Hydrogen Production with Tunable Nanorod Heterostructures. *J. Phys. Chem. Lett.* **2010**, *1*, 1051–1054.
27. Talapin, D. V.; Nelson, J. H.; Shevchenko, E. V.; Aloni, S.; Sadtler, B.; Alivisatos, A. P. Seeded Growth of Highly Luminescent CdSe/CdS Nanoheterostructures with Rod and Tetrapod Morphologies. *Nano Lett.* **2007**, *7*, 2951–2959.
28. Carbone, L.; Nobile, C.; De Giorgi, M.; Sala, F. D.; Morello, G.; Pompa, P.; Hytch, M.; Snoeck, E.; Fiore, A.; Franchini, I. R. et al. Synthesis and Micrometer-Scale Assembly of Colloidal CdSe/CdS Nanorods Prepared by a Seeded Growth Approach. *Nano Lett.* **2007**, *7*, 2942–2950.
29. Kreibig, U.; Vollmer, M. *Optical Properties of Metal Clusters*; Springer: Berlin, 1995.
30. Bohren, C. F.; Huffman, D. R. *Absorption and Scattering of Light by Small Particles*; Wiley: New York, 1998.
31. Del Fatti, N.; Christofilos, D.; Vallée, F. Optical Response of a Single Gold Nanoparticle. *Gold Bull.* **2008**, *41*, 147–158.
32. Klimov, V. I. Spectral and Dynamical Properties of Multiexcitons in Semiconductor Nanocrystals. *Annu. Rev. Phys. Chem.* **2007**, *58*, 635–673.
33. Klimov, V. I. Optical Nonlinearities and Ultrafast Carrier Dynamics in Semiconductor Nanocrystals. *J. Phys. Chem. B* **2000**, *104*, 6112–6123.
34. Langot, P.; Tommasi, R.; Vallée, F. Nonequilibrium Hole Relaxation Dynamics in an Intrinsic Semiconductor. *Phys. Rev. B* **1996**, *54*, 1775–1784.
35. Langot, P.; Del Fatti, N.; Christofilos, D.; Tommasi, R.; Vallée, F. Femtosecond Investigation of the Hot-Phonon Effect in GaAs at Room Temperature. *Phys. Rev. B* **1996**, *54*, 14487–14493.
36. Tommasi, R.; Langot, P.; Vallée, F. Femtosecond Hole Thermalization in Bulk GaAs. *Appl. Phys. Lett.* **1995**, *66*, 1361.
37. Horley, P. P.; Gorley, V. V.; Gorley, P. M.; Gonzalez-Hernandez, J.; Vorobiev, Y. V. On Correlation of CdS and CdSe Valence Band Parameters. *Thin Solid Films* **2005**, *480−481*, 373–376.
38. Zhu, H.; Song, N.; Rodríguez-Córdoba, W.; Lian, T. Wave Function Engineering for Efficient Extraction of up to Nineteen Electrons from one CdSe/CdS Quasi-Type II Quantum Dot. *J. Am. Chem. Soc.* **2012**, *134*, 4250–4257.
39. Del Fatti, N.; Vallée, F. Ultrafast Optical Nonlinear Properties of Metal Nanoparticles. *Appl. Phys. B: Laser Opt.* **2001**, *73*, 383–390.
40. Asbury, J. B.; Hao, E.; Wang, Y.; Ghosh, H. N.; Lian, T. Ultrafast Electron Transfer Dynamics from Molecular Adsorbates to Semiconductor Nanocrystalline Thin Films. *J. Phys. Chem. B* **2001**, *105*, 4545–4557.
41. Zhang, J. Z. Interfacial Charge Carrier Dynamics of Colloidal Semiconductor Nanoparticles. *J. Phys. Chem. B* **2000**, *104*, 7239–7253.
42. Kuang, D.; Ito, S.; Wenger, B.; Klein, C.; Moser, J.-E.; Humphry-Baker, R.; Zakeeruddin, S. M.; Grätzel, M. High Molar Extinction Coefficient Heteroleptic Ruthenium Complexes for Thin Film Dye-Sensitized Solar Cells. *J. Am. Chem. Soc.* **2006**, *128*, 4146–4154.
43. Moser, J. E. Dynamics of Interfacial and Surface Electron Transfer Processes. In *Dye-Sensitized Solar Cells*; Kalyanasundaram, K., Ed.; EPFL Press: Lausanne, 2010; pp 403−456.
44. Arbouet, A.; Voisin, C.; Christofilos, D.; Langot, P.; Del Fatti, N.; Vallée, F.; Lermé, J.; Celep, G.; Cottancin, E.; Gaudry, M.; et al. Electron-Phonon Scattering in Metal Clusters. *Phys. Rev. Lett.* **2003**, *90*, 177401.
45. Del Fatti, N.; Arbouet, A.; Vallée, F. Femtosecond Optical Investigation of Electron−Lattice Interactions in an Ensemble and a Single Metal Nanoparticle. *Appl. Phys. B: Laser Opt.* **2006**, *84*, 175–181.
46. Voisin, C.; Christofilos, D.; Loukakos, P.; Del Fatti, N.; Vallée, F.; Lermé, J.; Gaudry, M.; Cottancin, E.; Pellarin, M.; Broyer, M. Ultrafast Electron-Electron Scattering and Energy Exchanges in Noble-Metal Nanoparticles. *Phys. Rev. B* **2004**, *69*, 195416.
47. Baida, H.; Mongin, D.; Christofilos, D.; Bachelier, G.; Crut, A.; Maioli, P.; Del Fatti, N.; Vallée, F. Ultrafast Nonlinear Optical Response of a Single Gold Nanorod Near Its Surface Plasmon Resonance. *Phys. Rev. Lett.* **2011**, *107*, 057402.
48. Juvé, V.; Scardamaglia, M.; Maioli, P.; Crut, A.; Merabia, S.; Joly, L.; Del Fatti, N.; Vallée, F. Cooling Dynamics and Thermal Interface Resistance of Glass-Embedded Metal Nanoparticles. *Phys. Rev. B* **2009**, *80*, 195406.
49. Tiggesbäumker, J.; Köller, L.; Meiwes-Broer, K.-H. Bound-Free Collective Electron Excitations in Negatively Charged Silver Clusters. *Chem. Phys. Lett.* **1996**, *260*, 428–432.
50. Lermé, J.; Palpant, B.; Prével, B.; Pellarin, M.; Treilleux, M.; Vialle, J.-L.; Perez, A.; Broyer, M. Quenching of the Size Effects in Free and Matrix-Embedded Silver Clusters. *Phys. Rev. Lett.* **1998**, *80*, 5105–5108.
51. Lermé, J.; Baida, H.; Bonnet, C.; Broyer, M.; Cottancin, E.; Crut, A.; Maioli, P.; Del Fatti, N.; Vallée, F.; Pellarin, M. Size Dependence of the Surface Plasmon Resonance Damping in Metal Nanospheres. *J. Phys. Chem. Lett.* **2010**, *1*, 2922–2928.
52. Mulvaney, P.; Linnert, T.; Henglein, A. Surface Chemistry of Colloidal Silver in Aqueous Solution: Observations on Chemisorption and Reactivity. *J. Phys. Chem.* **1991**, *95*, 7843–7846.
53. Novo, C.; Funston, A. M.; Gooding, A. K.; Mulvaney, P. Electrochemical Charging of Single Gold Nanorods. *J. Am. Chem. Soc.* **2009**, *131*, 14664–14666.
54. Kamat, P. V. Manipulation of Charge Transfer Across Semiconductor Interface. A Criterion That Cannot Be Ignored in Photocatalyst Design. *J. Phys. Chem. Lett.* **2012**, *3*, 663–672.
55. Warren, S. C.; Walker, D. A.; Grzybowski, B. A. Plasmoelectronics: Coupling Plasmonic Excitation with Electron Flow. *Langmuir* **2012**, *28*, 9093–9102.
56. Dondapati, S. K.; Ludemann, M.; Müller, R.; Schwieger, S.; Schwemer, A.; Händel, B.; Kwiatkowski, D.; Djiango, M.; Runge, E.; Klar, T. A. Voltage-Induced Adsorbate Damping

of Single Gold Nanorod Plasmons in Aqueous Solution. *Nano Lett.* **2012**, *12*, 1247–1252.
57. Parkins, G.; Lawrence, W.; Christy, R. Intraband Optical Conductivity $\sigma(\omega,T)$ of Cu, Ag, and Au: Contribution from Electron-Electron Scattering. *Phys. Rev. B* **1981**, *23*, 6408–6416.
58. Johnson, P. B.; Christy, R. W. Optical Constants of the Noble Metals. *Phys. Rev. B* **1972**, *6*, 4370–4379.
59. Carbone, L.; Jakab, A.; Khalavka, Y.; Sönnichsen, C. Light-Controlled One-Sided Growth of Large Plasmonic Gold Domains on Quantum Rods Observed on the Single Particle Level. *Nano Lett.* **2009**, *9*, 3710–3714.